

Effective removal of Acetamiprid pesticide from wastewater using low-cost nano sorbent derived from *Moringa Oleifera* seeds: Adsorption kinetics and Isotherm.

Mai El-Kammah^{1*}, Maneea Moubarak²

¹Department of Natural Resources and Agricultural Engineering, Faculty of Agriculture, Damanhour University, Damanhour 22511, Egypt

²Departement of Horticulture, Faculty of Agriculture, Damanhour University, Damanhour 22511, Egypt

Abstract

*The highly toxic systemic neonicotinoid insecticide Acetamiprid may seriously damage aquatic ecosystems and human health when it reaches into water bodies. Therefore, there is an urgent need to create environmentally friendly, inexpensive, and efficient adsorbents to remove Acetamiprid from effluents. The current study presents research on converting *Moringa oleifera* seed waste (MOS) obtained from oil industry wastes into beneficial nano sorbent. In order to maximize the removal of Acetamiprid from contaminated wastewater, adsorption study examined the effects of solution pH, agitation time, Acetamiprid concentration, and temperature. The adsorption equilibrium was modeled with Langmuir isotherm. The adsorption kinetics was modeled with power function and Elovich equation. Depending on Langmuir models, maximum adsorption capacity for nano sorbent reached 70.22 mg·g⁻¹, which is 5.8 times higher than q_{max} of bulk MOS. According to the thermodynamic analysis, Acetamiprid adsorption occurs spontaneously and exothermically. The three main mechanisms of adsorption on nMOS were found to be hydrogen bonding, electrostatic interlinkage, and π - π interactions. The sorption capacity in the first four cycles of the adsorption-desorption investigated a slight decrease from 94% to 88%, indicating the effective reuse of nMOS in Acetamiprid removal from effluents. Overall, the experimental findings revealed that nMOS is a low-cost, environmentally friendly, and promising nanosorbent that may be used to treat Acetamiprid-contaminated effluents.*

Received 1st May 2024

Revised 14th October 2024

Accepted 13th November 2024

Keywords

Neonicotinoid; Acetamiprid;

Adsorption; kinetic

Mechanism of adsorption

1. Introduction

Continuous and indiscriminate exposure of pesticides in different agricultural activities has led to undesired environmental contamination. Neonicotinoids, a type of pesticide commonly used in agriculture, have been particularly controversial due to their harmful effects on pollinators such as bees. Studies have shown that neonicotinoids can impair bee navigation, reproduction, and overall health, posing a serious threat to the stability of ecosystems and food production. In response to this issue, many countries have started to restrict or ban the use of neonicotinoids, emphasizing the need

*Correspondence author: Mai_elkammah@agr.dmu.edu.eg

<https://doi.org/10.21608/auber.2024.286645.1079>

This is an open access article under the CC BY-NC-ND license (<http://creativecommons.org/licenses/by-nc-nd/4.0/>).

for more sustainable and eco-friendly farming practices [1], [2]. Acetamiprid is a neonicotinoid insecticide that is commonly used in agriculture to control pests. It works by interfering with the nervous system of insects, causing paralysis and eventually death. Due to its effectiveness and relatively low toxicity to mammals, Acetamiprid has become a popular choice among farmers. However, there have been growing concerns about its impact on pollinators, particularly bees, as studies have shown that it can be harmful to their health and contribute to their decline. As a result, there is an ongoing debate about the continued use of Acetamiprid and the need for more sustainable alternatives in pest control bodies [3]. Due to its long half life (DT50), Acetamiprid remains active in the environment for an extended period of time. This allows for prolonged control of insect pests, reducing the need for frequent reapplication [4], [5], [6]. Nowadays, nanomaterials are employed to capture and remove neonicotinoids at the molecular level. This approach offers a highly efficient and cost-effective solution for the removal of these harmful pesticides from wastewater [7], [8]. Application of nanosized materials in remediation of wastewater has gained much attention due to their unique physicochemical characteristics such as small sizes (<100 nm), high specific surface areas, high adsorption capacities and reactivity resulting in enhanced performance over their bulk counterparts. *Moringa oleifera* seeds are an effective and low-cost method used in water treatment plants to remove impurities and purify the water. These seeds contain natural coagulants that can bind together particles and suspended solids in the water, making it easier to filter and remove them. The seeds are crushed and added to the water, allowing the coagulants to work their magic. This simple and cost-effective method has been proven to be highly effective in improving water quality, especially in areas where access to clean drinking water is limited. Furthermore, the use of *Moringa oleifera* seeds in water treatment is environmentally friendly as it does not introduce harmful chemicals into the water supply. Additionally, the affordability of *Moringa oleifera* seeds makes this method sustainable and accessible for communities with limited resources, ensuring a consistent supply of clean and safe drinking water for those in need. This method has the potential to greatly improve public health and reduce waterborne diseases. Different studies have reported the potential of several sorbents for acetamiprid removal. (Paramasivan et al., 2019) [9] has found that, acetamiprid removal efficiency onto Graphene magnetic nanoparticle was 72% and (Choumane et al., 2016) [10] reported that the low adsorption capacity for bentonite clay, and kaolin in removing Acetamiprid could be explained by the low specific surface area for them. While (Cobas et al., 2016) [11] evaluated the potentials of a cheap biosorbent (chestnut shells) for the removal of acetamiprid, the reports described the applicability of the biosorbent in eliminating acetamiprid pesticide. The adsorption processes were best explained by pseudo-second-order and Freundlich isotherm kinetic models. Mesoporous activated carbon from starch (ACS) was applied to remove pesticides from wastewater [12]. The adsorption study conducted by (Lu et al., 2022) [13] showed that the use of activated carbon as a sorbent achieved an even higher acetamiprid removal efficiency of 85%. These findings highlight the importance of exploring different sorbents for the effective removal of acetamiprid from water sources. Ball mill is grinding technique that is used to reduce the particle size of materials. It is commonly used in industries such as mining, construction, and ceramics. The grinding media inside the ball mill can be made of steel, ceramic, or even rubber, depending on the material being processed. The size of the balls and the speed of rotation can be adjusted to achieve the desired fineness of the final product. Overall, the ball mill is a versatile and efficient tool for grinding and pulverizing materials. Due to the high efficiency of nano particles, we have hypothesized that synthesis of nano-adsorbent using the priceless byproduct moringa seeds wastes would greatly enhance the capacity of bulk counterpart for removal of an emerging contaminant from wastewater. The proposed nano-moringa oleifera seeds (nMOS) adsorbent is novel, green, effective and low-cost nanomaterial and a

substitute of expensive, restricted and inefficient methods such as irradiation, coagulation, ion exchange, physical treatments, flocculation, chemical precipitation and electrochemical destruction [14], [15], [16], [17].

The current study aims to explore the adsorption capacity of nMOS and assess their effectiveness in removing Acetamiprid from wastewater. By comparing the results with previous studies, a comprehensive understanding of the adsorption behavior of Acetamiprid can be achieved, leading to the development of more efficient treatment methods for its removal from wastewater. Furthermore, synthesis and application of nMOS as a low-cost solution to generate green nano-sorbents from invaluable materials would exhibit a precise role in the environmental remediation and the global environmental challenge issue.

1. Methods and tools

1.1. Nano-sized MOS (nMOS) adsorbent

Moringa oleifera seeds (MOS) were procured from Ministry of Agriculture - Cairo. Solvent extraction method was used to extract the oil from the moringa seeds [18]. The resultant material is defined as (press cake), which is the residuals of the seeds after oil extracting process. The press cake was oven dried at 60 °C for 1 h to get rid of any excess solvent. After this step, dried Moringa seeds were crushed and passed through two different sieves. The first sieve mesh was 2 mm. The proportion that was passed through the 2 mm sieve was determined as Bulk Moringa oleifera seeds (bMOS). A fraction of bMOS was passed through the second sieve which was 51- μ m. Passed particles were mechanically ground using the precision ball mill (Fritsch, Germany) to diminish particle size less than 100 nm following the method reported by Elkhatib et al., 2015 [19]. Fritsch Planetary Mono Mill Pulverisette 6 classic line equipped with 80-ml stainless steel grinding bowl and 150 g of 1 mm steel grinding balls. The grinding process was performed at 650 rpm disk speed for 75 min. To maintain an optimum viscosity for grinding, 48 ml of isopropyl alcohol were added to the sample. The samples were ground in cycles in which 3 min grinding time is followed by a programmed pausing time of 10 min to avoid over pressure. After several (3) cycles, the outside temperature of the bowl was checked (below 70 °C). The characteristics of the ground samples were investigated using scanning electron microscopy combined with energy-dispersive X-ray spectroscopy (SEM-EDX,) and Fourier transmission infra-red (FTIR) analysis.

1.2. Characterization of Acetamiprid

The commercial formulation of Acetamiprid was purchased from Syngenta Agro (Egypt). Stock solution of (1000 mg/l) was prepared and kept in darkness. Serial dilution with deionized water was used to obtain the desired range of concentrations. To detect the maximum wavelength for Acetamiprid determination, spectrophotometric measurements were performed in the range 190–400 nm using GENESYS 10S UV-Vis Spectrophotometer. Full scan spectrum was obtained with λ max at 245 nm [10], [20]. 5 Standard solutions for the calibration curves were prepared by the stepwise dilution of the stock solution to obtain concentrations in the range of 1:50 mg/l.

2.3. Adsorption studies

The adsorption tests of Acetamiprid on bMOS and nMOS were performed by mixing 0.1 g of adsorbent with 40 mL of Acetamiprid solution. The mixtures were shaken at 160 rpm for a maximum of 24 h at 25°C. At the end of the test, the suspension was centrifuged at 4000 rpm (1800 g) for 5 min and the supernatant was filtered using a 0.45 μ m membrane. The final concentration in the supernatant was determined by UV-Vis spectrophotometry at 245 nm.

The percentage of Acetamiprid removal from aqueous solution was calculated according to equation

$$\text{Removal (\%)} = ((C_0 - C_e) / C_0) * 100 \quad [\text{eq.1}]$$

Where C_0 is the initial concentration in mgL^{-1} , C_e is the final concentration in mgL^{-1} .

The adsorption capacity (q_e) of the adsorbent in equilibrium with the liquid phase was calculated using equation 2

$$q_e (\text{mg} \cdot \text{g}^{-1}) = (C_0 - C_e) \cdot V / m \quad [\text{eq.2}]$$

Where V is the liquid phase volume expressed in L and m is the adsorbent mass expressed in g.

Various adsorption tests of Acetamiprid on MOS adsorbent were designed and performed to determine the influence of contact time (5 - 120 min), pH solution (pH=2-11), MOS adsorbent dose (0.1- 0.4 g), temperature (298.15 – 318.15 K) and initial concentrations (10 - 400 mgL^{-1}), in the adsorption equilibrium, adsorption kinetics and thermodynamics.

3. Results and Discussion

3.1. Characterization of nMOS

Figure (1A) revealed scanning electron microscopy (SEM) image of nMOS which showed a smooth morphology devoid of surface breaks. Particle structures appeared significant change after adsorption on nMOS (Fig. 1B). There were lots of pores and tiny spherical forms. Several agricultural adsorbents, including orange peel [21] and wheat straw [22] have been reported in the literature to exhibit comparable surface changes affected by adsorption processes. The elemental composition of nMOS both before and after adsorption was determined using the EDS analysis. Certain elements, like carbon (55.68%), oxygen (33.96%), and nitrogen (9.45%), had high percentages in the results, while other elements had relatively low percentages such as sulfur (0.59%), phosphorus (0.26%), and calcium (0.07%) . Depending on sorption process, higher percentages of calcium (0.12%), oxygen (34.10%), and nitrogen (13.43%) were found in nMOS confirming the Acetamiprid sorption on nMOS. The Fourier-transform infrared spectroscopy (FTIR) spectra of nMOS before adsorption was analyzed , the active band at 3375.5 cm^{-1} is related to $-\text{OH}$ and $-\text{NH}_2$ stretching vibration present in lignin, proteins, carbohydrates, fatty acids, while the band at 2926.5 cm^{-1} is related to the aliphatic $\text{C}-\text{H}$ group [23]. The strong peak at 1656.87 cm^{-1} is corresponded to the $\text{C}-\text{O}$ bond of amides or $\text{N}-\text{H}$ bending in proteins[24], [25] , whereas the bands at 1540.51 and 1060.19 cm^{-1} can be related to $\text{C}=\text{O}$ stretch (Chaari et al., 2019; Fernandez et al., 2015b). The FTIR spectrum of Acetamiprid loaded nMOS has shown changes in the peak intensity and wave number. The changes in wave number and peak intensity reveal the interaction of Acetamiprid and the function groups of moringa such as $-\text{OH}$ bond, $\text{C}-\text{H}$ group, $\text{C}-\text{O}$ bonds of amides and $\text{N}-\text{H}$ groups in carbohydrates, fatty acids and proteins . These functional groups have a main role in the adsorption reaction [26], [27].

3.2. Acetamiprid adsorption isotherms

To comprehend and interpret the adsorption process, the Acetamiprid adsorption process on bMOS and nMOS must be represented using adsorption isotherm models. Six adsorption isotherm models were used to calculate isotherm parameters. Best fitted models for experimental data are shown in Table (1). The Langmuir model with lower standard error (SE) values and higher R^2 values demonstrated that the Acetamiprid adsorption by bMOS and nMOS adhered to the model (Fig. 2). According to the Langmuir isotherm, the maximum adsorption capacity (q_{max}) was determined to be 70.22 mgg^{-1} for nMOS and 12.00 mgg^{-1} for bMOS. For Acetamiprid , the nMOS q_{max} value was

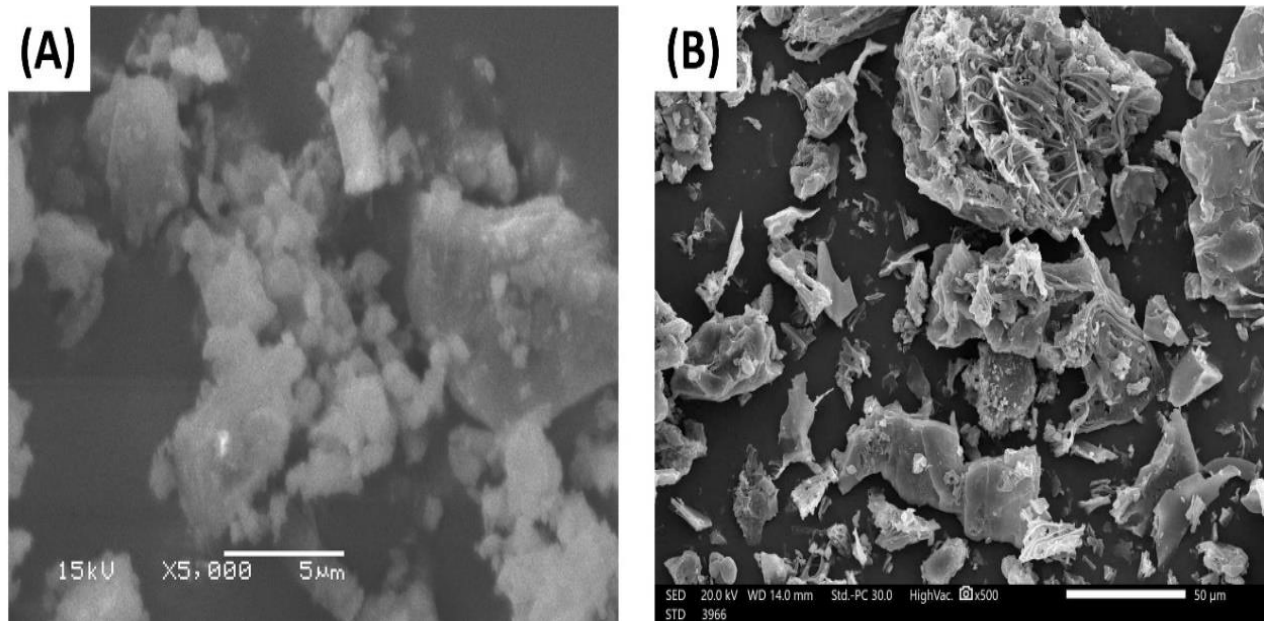


Fig.1 Scanning Electron microscope for a) nMOS before adsorption and b) nMOS after adsorption.

5.8 times greater than the bMOS value. The greater nMOS specific surface area can explain the enrichment in adsorption capacity. (Table 2) illustrates the maximum adsorption capacity for several sorbent materials in adsorption neonicotinoid and similar pesticides. This study reported high adsorption capacity comparing with other studies due to high specific surface area for nMOS $4.6 \text{ m}^2 \text{ g}^{-1}$ as reported in previous study [28]. (Choumane et al., 2016) [10] reported that the low adsorption capacity for bentonite clay, and kaolin could be explained by the low specific surface area for them. The fact that Langmuir isotherm fits the experimental data very well confirms the monolayer coverage of Acetamiprid onto MOS nano particles ($q_m = 70.22 \text{ mg/g}$) and also the homogeneous distribution of active sites on the adsorbent, since the Langmuir equation assumes that the surface is homogeneous. This suggests that the Acetamiprid molecules are uniformly adsorbed onto nMOS, forming complete monolayer coverage. The value of q_m , which represents the maximum adsorption capacity, further reinforces the idea that all available active sites on nMOS surface are occupied by the pesticide molecules.

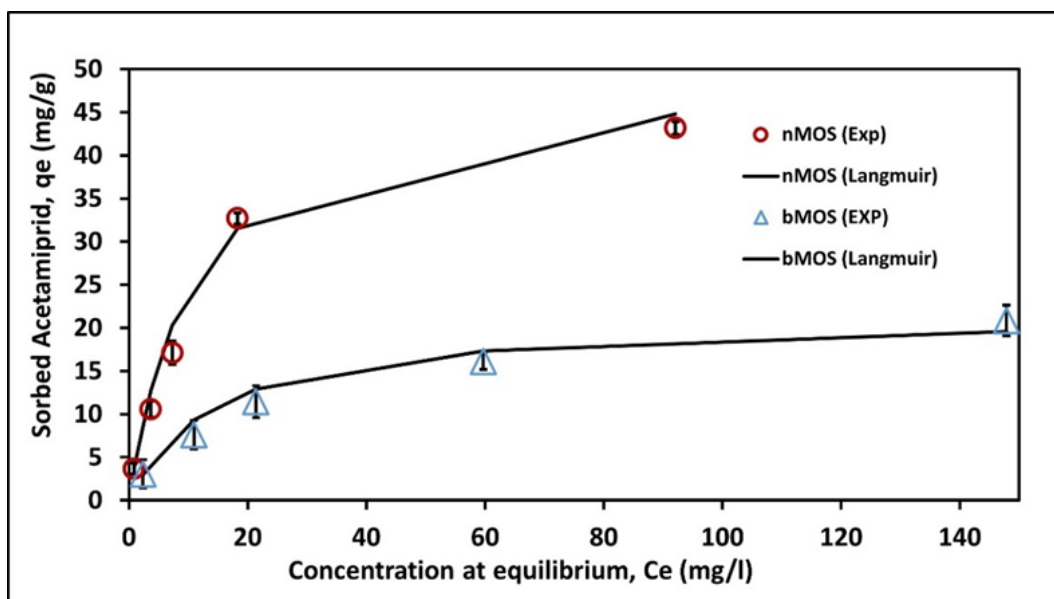


Fig.2 Langmuir isotherm for Acetamiprid adsorption onto nMOS.

Table 1. Sorption isotherm models for Acetamiprid adsorption by nMOS and bMOS.

Adsorption isotherms	Description	Parameters	nMOS	bMOS
Freundlich $q_e = K_F C_e^{1/n}$	K_F = constant of Freundlich (the adsorption volume of the adsorbent) n = constant (intensity of the analyte sorption)	K_F (mL/g) $1/n$ R^2 SE	1.6061 0.5411 0.9335 0.2919	2.3419 0.4647 0.9708 0.1482
Langmuir $q_e = \frac{q_{max} K_L C_e}{1 + K_L C_e}$	q_{max} = maximum adsorption capacity K_L = constant of Langmuir (free energy of adsorption)	q_{max} (mg/g) K_L (L/mg) R^2 SE	40.22 0.0934 0.9953 0.0082	12.00 0.0788 0.9908 0.0125
Temkin $\theta = \frac{RT}{\Delta Q} \ln K_0 C_e$	ΔQ = variation of adsorption energy ($-\Delta H$) K_0 = constant of Temkin T = temperature (K) R = universal gas constant.	ΔQ (J/mol) K_0 (L/mg) R^2 SE	13667.0 1.2914 0.9554 0.0791	16503.1 0.6993 0.9847 0.009

Table 2. Maximum adsorption capacity for different sorbents in removing neonicotinoids pesticides.

Sorbents	Pesticide	Adsorption capacity	References
Sludge-Based Activated Carbons	Thiamethoxam	126.8	[29]
Granular activated carbon	Thiamethoxam	60 mg/g	[30]
Ricinodendron heudelotii shells	Imidacloprid	43.48 mg/g	[31]
Peanut shell	Imidacloprid	8.68 mg/g	[32]
Tangerine peels	Acetamiprid	35.70 mg/g	[33]
Bentonite clay	Acetamiprid	9.17 mg/g	[34]
Kaoline	Acetamiprid	7.85 mg/g	[34]
magnetic copper-based metal–organic framework	Thiamethoxam	2.88 mg/g	[35]
Nano Moringa Oleifera sedes. nMOS	Acetamiprid	70.22 mg/g	This work
Bulk Moringa Oleifera sedes	Acetamiprid	12	This work

Additionally, the good fit of the Langmuir isotherm indicates that there is no preferential adsorption occurring on specific regions of the adsorbent, further supporting the hypothesis of a homogeneous distribution of active sites. According to R_L value, the isotherms' shapes can be classified as irreversible when ($RL = 0$), favorable ($0 < RL < 1$), linear ($RL = 1$), unfavorable ($RL > 1$), or favorable ($0 < RL < 1$). R_L is a dimensionless constant called separation factor or equilibrium parameter which is defined by the following equation $R_L = \frac{1}{1 + K_L C_0}$ Where C_0 (mg/L) is the initial pesticide concentration and K_L (L/mg) is the Langmuir constant related to the energy of adsorption. In this study, the R_L values for the nMOS. Acetamiprid interactions were found to be within the range of 0-1, indicating a favorable uptake of the Acetamiprid process. This suggests that the adsorption of Acetamiprid onto the nMOS surface is thermodynamically feasible and that the system is reversible to some extent.

3.3. Optimization of parameters affecting Acetamiprid removal by nMOS.

3.3.1. Contact time: The contact time refers to the duration that the adsorbent and the adsorbate are in contact with each other. By increasing the contact time, more adsorbate molecules can come into contact with the adsorbent surface, leading to increased adsorption efficiency. This allows for a higher removal rate of pollutants or contaminants from the solution. Therefore, optimizing the contact time plays a crucial role in maximizing the adsorption performance and ensuring effective purification or separation processes. The impact of contact duration on the Acetamiprid adsorption by nMOS was investigated at $100 \text{ mg}\cdot\text{L}^{-1}$ for a duration of 5 minutes to 24 hours. During the first fifteen minutes, the adsorption of Acetamiprid on nMOS proceeded very quickly and tended toward the equilibrium plateau (Fig. 3). Within 30 minutes, approximately 93% of Acetamiprid on nMOS had been removed, bringing the maximum adsorption capacity to a close.

3.3.2. Adsorbent dose: The adsorbent dose greatly affects the total specific surface area and binding sites of the adsorbent. The influence of nMOS adsorbent dose (0.10-0.40 g) on the Acetamiprid removal was examined. The results showed that increasing the adsorbent dose has led to a significant increase in the total specific surface area and binding sites availability for adsorption. This, in turn, resulted in a higher efficiency of removal. At the lowest adsorbent dose of 0.10 g, removal efficiency was found to be relatively low, indicating that there were limited binding sites available for adsorption. However, as the adsorbent dose was increased to 0.20 g, the Acetamiprid removal efficiency improved significantly, suggesting that a higher dosage of adsorbent led to a greater number of binding sites for the pesticide molecules to attach to.

3.3.3. Effect of solution pH: The pH of the liquid phase is a crucial parameter that effects adsorption behavior because of the major influence of the pH on ionization of functional groups and adsorbate surface charge [36], [37]. At low pH values, functional groups may be protonated and carry a positive charge, leading to repulsion between the adsorbate and the adsorbent surface. On the other hand, at high pH values, functional groups may be deprotonated and carry a negative charge, facilitating the attraction between the two. Therefore, the pH of the liquid phase must be carefully controlled to optimize the adsorption process and ensure efficient removal of ions from the solution [38]. Numerous tests were conducted at various pH values between pH 2 and pH 11 in order to investigate the effect of solution pH on the adsorption process. The results of the experiment showed that the maximum nMOS removal capacity (93%) was reached at $\text{pH} = 4$ (Fig. 3). However when pH value increased up to 6, removal efficiency decreased.

3.3.4. Adsorption kinetics

The findings resulted from the study of adsorption kinetics of nMOS for Acetamiprid removal at various time intervals are displayed in (Fig4). After the first fifteen minutes, the rate of adsorption process was quite rapid. After that, it started to slow down and achieved equilibrium after thirty minutes, removing about 93% of the Acetamiprid. Four kinetic models were fitted to the adsorption kinetic data. Table (3) contains a list of the parameters and the kinetic models. The high standard error (SE) indicates that neither the parabolic diffusion model nor the first order model accurately represented the adsorption kinetics. On the other hand, the power function kinetic model and the Elovich model displayed the lowest SE values and the highest determination coefficients (R^2) represented best fitted for kinetics data (fig.4).

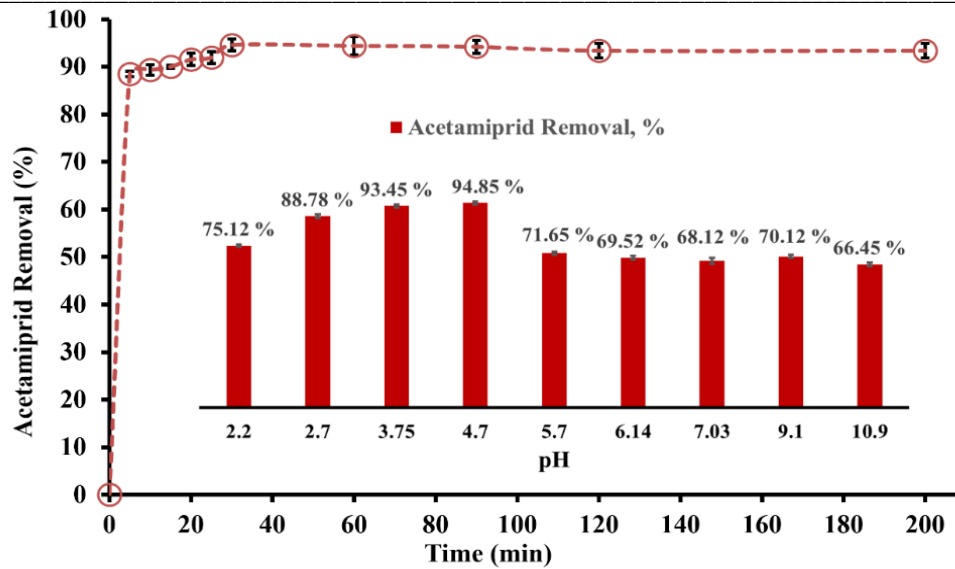


Fig.3 Effect of contact time and pH on removal Acetamiprid efficiency

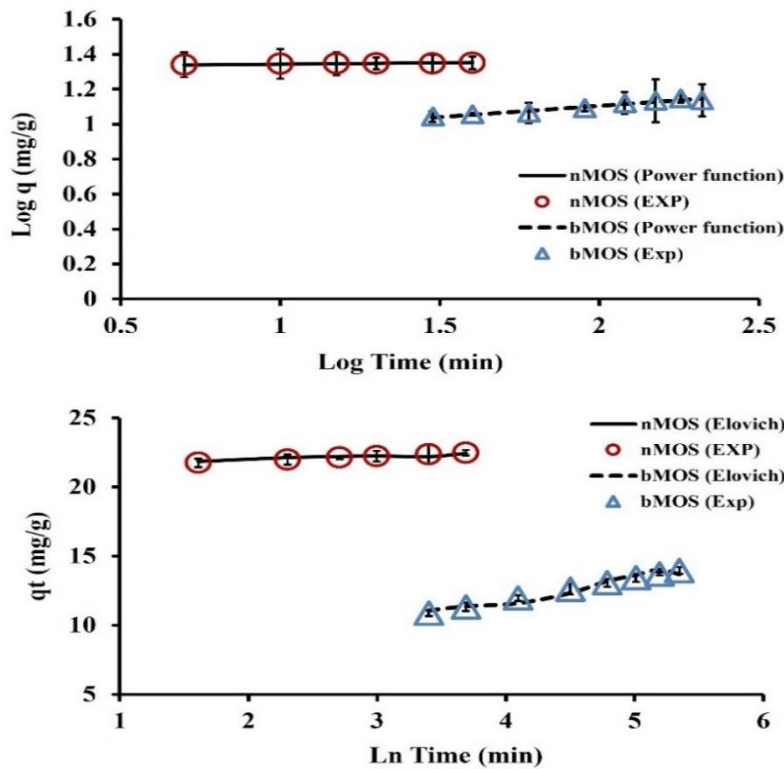


Fig.4 Kinetics model for adsorption Acetamiprid onto nMOS

Table 3. Kinetics models parameters for Acetamiprid adsorption by nMOS and bMOS.

Adsorption kinetic model	Description	Parameters	Adsorbent	
			nMOS	bMOS
Elovich $q_t = \frac{1}{\beta} \ln(1 + \alpha\beta t)$	β = constant related to the extent of surface coverage α = the initial adsorbed rate	α (mg/ g min)	1.1380	0.3781
		β (mg/g)	0.2273	0.7521
		R^2	0.9895	0.9810
		SE	0.5508	0.7451
Power function $q = k_p C_0 t^{1/m}$	k_p = apparent adsorbed rate coefficient $1/m$ = constant. C_0 = initial concentration of Acetamiprid	k_p (min^{-1})	0.9987	0.9930
		$1/m$	0.6047	0.5919
		R^2	0.9151	0.9535
		SE	0.0972	0.0689

The power function model parameters (k_a and $1/m$) were calculated from the slope and the intercept of the linear plots ($\log q$ versus $\log t$). The SE values of the power function model were much lower than the SE values of the Elovich kinetic model, which indicate that kinetics of Acetamiprid can be best described by the power function kinetic model, as shown in table 3. The effectiveness of nMOS in removing Acetamiprid can be compared using the desorption rate parameter (k_p) of the power function model. Elovich equation plots of adsorption Acetamiprid exhibited linear relationships exist between " qt " and " $\ln t$ ". The Elovich equation parameters, α and β were calculated from the slope and intercept of the linear plots and reported in Table (2). The amount of Acetamiprid adsorbed by nMOS is higher than that adsorbed by bMOS. According to (Fouad, 2023) [39] α constant represents the chemisorption rate at zero coverage and β based on the extent of surface coverage and chemisorption activation energy. The Elovich equation is fit with experimental adsorption data for nMOS more than bMOS, as indicated by higher values of α constant related to the adsorption rate.

3.4. Adsorption Thermodynamics

The thermodynamic parameters of Acetamiprid sorption: Gibbs free energy (ΔG°), enthalpy (ΔH°) and entropy (ΔS°) are crucial in understanding the driving forces and feasibility of sorption process. ΔG° provides information about the spontaneity of the sorption reaction, where a negative value indicates a favorable process. ΔH° represents the heat exchange during the sorption, while ΔS° reflects the change in randomness of the system. These thermodynamic parameters help in predicting the conditions required for efficient sorption and provide insights into the overall stability and energetics of the system adsorbent [40], [41]. Overall, understanding these parameters is essential for the successful design and implementation of efficient sorption systems. Next equations were used to calculate the parameters of thermodynamics. Higher temperatures result in less effective removal by nMOS, as indicated by the increasing (negative) ΔG° values. The adsorption of Acetamiprid rises with temperature, indicating that adsorption process is exothermic, as indicated by the negative magnitude of enthalpy change (ΔH).

$$\Delta G = -RT \ln K_c \quad [\text{eq. 3}]$$

$$\ln K_c = \Delta S^\circ/R - \Delta H^\circ/RT \quad [\text{eq. 4}]$$

Where K_c is equilibrium constant obtained by the Langmuir equation ($K_c = q_e/C_e$ at 298 – 318 K), R is the gas constant ($8.314 \text{ J}\cdot\text{mol}^{-1}\cdot\text{K}^{-1}$), and T is temperature expressed in Kelvin.

3.5. Proposed mechanism

Three main interactions between Acetamiprid and nMOS have been proposed: (1) π - π interaction, (2) electrostatic interactions, and (1) hydrogen bonding. (1) Hydrogen bonding interaction: Since Acetamiprid contains O (strong H donors) and the nMOS H acceptor (OH) contains OH groups, it is suggested that a hydrogen bond will form between Acetamiprid strong H donor and the nMOS H acceptor. (2) Electrostatic interactions: The positively charged adsorbent functional groups on the surface of nMOS interact with the negatively charged binding sites of Acetamiprid. (3) The π - π interaction: Oxygen molecules on the surface of nMOS operate as electron donors because the material's surface is relatively rich in π electrons. Therefore, the π - π interaction between the π electron on the nMOS surface and the π electron cloud of Acetamiprid molecules may occur.

3.6. Reusability of nMOS for Acetamiprid removal

Reusability of nMOS is important for economic and practical application of the adsorption process. Thus, sequential batch adsorption-desorption tests were performed to assess nMOS reusability.

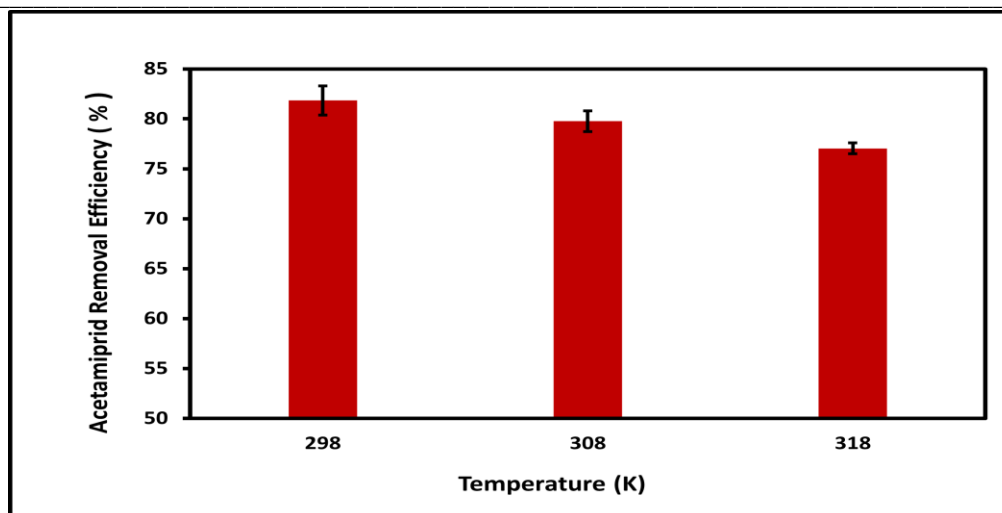


Fig.5 Effecting of temperature on removal efficiency.

The tests involved subjecting the nMOS to multiple cycles of adsorption and desorption, mimicking real-world scenarios. The experiment was conducted in triplicate, combining 0.1 g of nMOS with 20 mL of pesticide solution and shaking for half an hour. After centrifuging the mixture, the concentration of Acetamiprid in the supernatant was measured. Acetamiprid was desorbed with the addition of 20 mL of deionized water after the supernatant solution was discarded. There were five iterations of this technique (Fig. 5). For five consecutive cycles, the adsorption-desorption procedures were carried out repeatedly. The results showed that the nMOS maintained its adsorption capacity even after several cycles, indicating its potential for long-term use. This finding is significant as it allows for cost-effective and sustainable implementation of the adsorption process in various industries.

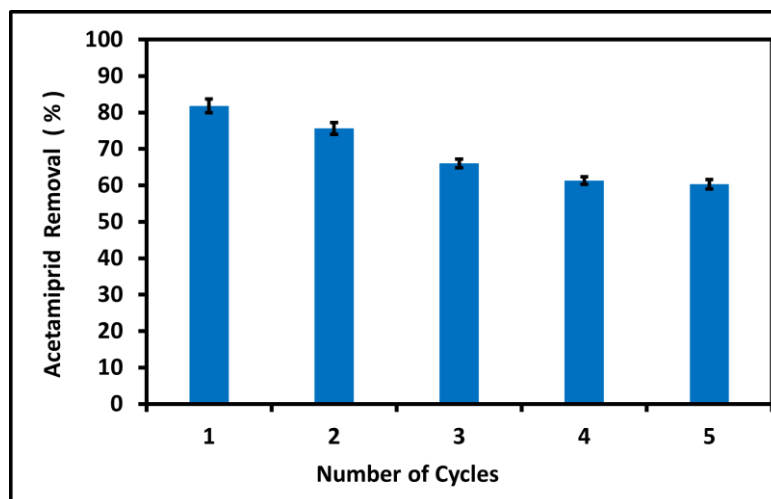


Fig.5 Sorption - Desorption tests for nMOS after 5 sorption cycles

Conclusion

The effective production and application of a nanomaterial obtained from the waste of Moringa oleifera seeds (nMOS) for the removal of Acetamiprid pesticides from effluents. Both of Langmuir model isotherm and power function model fitted well the adsorption data. Furthermore, the thermodynamic analysis indicated that the adsorption process is exothermic, spontaneous, and beneficial. Proposed adsorption processes for Acetamiprid adsorption on nMOS included electrostatic

interactions between the adsorbate and the adsorbent (nMOS), as well as π - π and hydrogen bonding. After five consecutive cycles, high removal efficiency of nMOS reduced slightly, indicating outstanding reusability for nano sorbent. The results of this study demonstrated the high potential of MOS nanoparticles for wastewater remediation.

References

- [1] J. E. Casida and K. A. Durkin, "Neuroactive insecticides: targets, selectivity, resistance, and secondary effects," *Annu Rev Entomol*, vol. 58, pp. 99–117, 2013.
- [2] N. Simon-Delso *et al.*, "Systemic insecticides (neonicotinoids and fipronil): trends, uses, mode of action and metabolites," *Environmental Science and Pollution Research*, vol. 22, no. 1, pp. 5–34, 2015.
- [3] K. L. Klarich *et al.*, "Occurrence of neonicotinoid insecticides in finished drinking water and fate during drinking water treatment," *Environ Sci Technol Lett*, vol. 4, no. 5, pp. 168–173, 2017.
- [4] D. Gibbons, C. Morrissey, and P. Mineau, "A review of the direct and indirect effects of neonicotinoids and fipronil on vertebrate wildlife," *Environmental Science and Pollution Research*, vol. 22, no. 1, pp. 103–118, 2015.
- [5] D. Goulson, "An overview of the environmental risks posed by neonicotinoid insecticides," *Journal of Applied Ecology*, vol. 50, no. 4, pp. 977–987, 2013.
- [6] K. Starner and K. S. Goh, "Detections of the neonicotinoid insecticide imidacloprid in surface waters of three agricultural regions of California, USA, 2010–2011," *Bull Environ Contam Toxicol*, vol. 88, no. 3, pp. 316–321, 2012.
- [7] J. Theron, J. A. Walker, and T. E. Cloete, "Nanotechnology and water treatment: applications and emerging opportunities," *Crit Rev Microbiol*, vol. 34, no. 1, pp. 43–69, 2008.
- [8] W. Zhang, "Nanoscale iron particles for environmental remediation: an overview," *Journal of nanoparticle Research*, vol. 5, no. 3, pp. 323–332, 2003.
- [9] T. Paramasivan *et al.*, "Graphene family materials for the removal of pesticides from water," *A new generation material graphene: applications in water technology*, pp. 309–327, 2019.
- [10] F. Z. Choumane and B. Benguella, "Removal of acetamiprid from aqueous solutions with low-cost sorbents," *Desalination Water Treat*, vol. 57, no. 1, pp. 419–430, 2016.
- [11] M. Cobas, J. Meijide, M. A. Sanromán, and M. Pazos, "Chestnut shells to mitigate pesticide contamination," *J Taiwan Inst Chem Eng*, vol. 61, pp. 166–173, 2016.
- [12] F. Suo *et al.*, "Mesoporous activated carbon from starch for superior rapid pesticides removal," *Int J Biol Macromol*, vol. 121, pp. 806–813, 2019, doi: <https://doi.org/10.1016/j.ijbiomac.2018.10.132>.
- [13] J. Lu, Z. Zhang, X. Lin, Z. Chen, B. Li, and Y. Zhang, "Removal of imidacloprid and acetamiprid in tea (*Camellia sinensis*) infusion by activated carbon and determination by HPLC," *Food Control*, vol. 131, p. 108395, 2022.
- [14] E. Elkhatib, M. Moharem, and A. Mahmoud, "Low cost nanoparticles derived from nitrogen fertilizer industry waste for the remediation of copper contaminated soil and water," *Environmental Engineering Research*, vol. 25, no. 6, pp. 930–937, 2020.
- [15] E. Elkhatib, M. Moharem, and H. Hamadeen, "Low-cost and efficient removal of mercury from contaminated water by novel nanoparticles from water industry waste," *Desalin. Water Treat*, vol. 144, pp. 79–88, 2019.
- [16] E. Elkhatib, M. Moharem, A. Mahdy, and M. Mesalem, "Sorption, release and forms of mercury in contaminated soils stabilized with water treatment residual nanoparticles," *Land Degrad Dev*, vol. 28, no. 2, pp. 752–761, 2017.
- [17] M. Moharem, E. Elkhatib, and M. Mesalem, "Remediation of chromium and mercury polluted calcareous soils using nanoparticles: Sorption–desorption kinetics, speciation and fractionation," *Environ Res*, vol. 170, pp. 366–373, 2019.
- [18] F. Anwar, M. Ashraf, and M. I. Bhangar, "Interprovenance variation in the composition of *Moringa oleifera* oilseeds from Pakistan," *J Am Oil Chem Soc*, vol. 82, no. 1, pp. 45–51, 2005.
- [19] E. Elkhatib, A. Mahdy, F. Sherif, and H. Hamadeen, "Evaluation of a novel water treatment residual nanoparticles as a sorbent for arsenic removal," *J Nanomater*, vol. 2015, 2015.
- [20] S. Li, X. Ma, Y. Jiang, and X. Cao, "Acetamiprid removal in wastewater by the low-temperature plasma using dielectric barrier discharge," *Ecotoxicol Environ Saf*, vol. 106, pp. 146–153, 2014, doi: <https://doi.org/10.1016/j.ecoenv.2014.04.034>.
- [21] M. E. Fernandez, B. Ledesma, S. Román, P. R. Bonelli, and A. L. Cukierman, "Development and characterization of activated hydrochars from orange peels as potential adsorbents for emerging organic contaminants," *Bioresour Technol*, vol. 183, pp. 221–228, 2015.
- [22] R. Han, L. Zhang, C. Song, M. Zhang, H. Zhu, and L. Zhang, "Characterization of modified wheat straw, kinetic and equilibrium study about copper ion and methylene blue adsorption in batch mode," *Carbohydr Polym*, vol. 79, no. 4, pp. 1140–1149, 2010.

- [23] N. Feng, X. Guo, S. Liang, Y. Zhu, and J. Liu, "Biosorption of heavy metals from aqueous solutions by chemically modified orange peel," *J Hazard Mater*, vol. 185, no. 1, pp. 49–54, 2011.
- [24] V. O. Arief, K. Trilestari, J. Sunarso, N. Indraswati, and S. Ismadji, "Recent progress on biosorption of heavy metals from liquids using low cost biosorbents: characterization, biosorption parameters and mechanism studies," *CLEAN–Soil, Air, Water*, vol. 36, no. 12, pp. 937–962, 2008.
- [25] A. Çelekli, M. Yavuzatmaca, and H. Bozkurt, "Kinetic and equilibrium studies on the adsorption of reactive red 120 from aqueous solution on *Spirogyra majuscula*," *Chemical Engineering Journal*, vol. 152, no. 1, pp. 139–145, 2009.
- [26] C. S. T. Araújo, E. I. Melo, V. N. Alves, and N. M. M. Coelho, "Moringa oleifera Lam. seeds as a natural solid adsorbent for removal of AgI in aqueous solutions," *J Braz Chem Soc*, vol. 21, no. 9, pp. 1727–1732, 2010.
- [27] C. S. T. Araújo *et al.*, "Bioremediation of waters contaminated with heavy metals using Moringa oleifera seeds as biosorbent," *Applied bioremediation-active and passive approaches*, vol. 23, pp. 227–255, 2013.
- [28] M. El-Kammah, E. Elkhatab, S. Gouveia, C. Cameselle, and E. Aboukila, "Enhanced removal of Indigo Carmine dye from textile effluent using green cost-efficient nanomaterial: Adsorption, kinetics, thermodynamics and mechanisms," *Sustain Chem Pharm*, vol. 29, no. June, p. 100753, 2022, doi: 10.1016/j.scp.2022.100753.
- [29] E. Sanz-Santos, S. Álvarez-Torrellas, L. Ceballos, M. Larriba, V. I. Águeda, and J. García, "Application of Sludge-Based Activated Carbons for the Effective Adsorption of Neonicotinoid Pesticides," *Applied Sciences*, vol. 11, no. 7, p. 3087, 2021.
- [30] D. T. Webb, M. R. Nagorzanski, M. M. Powers, D. M. Cwiertny, M. L. Hladik, and G. H. LeFevre, "Differences in Neonicotinoid and Metabolite Sorption to Activated Carbon Are Driven by Alterations to the Insecticidal Pharmacophore," *Environ Sci Technol*, vol. 54, no. 22, pp. 14694–14705, 2020.
- [31] K. Y. Urbain *et al.*, "Removal of imidacloprid using activated carbon produced from ricinodendron heudelotii shells," *Bull Chem Soc Ethiop*, vol. 31, no. 3, pp. 397–409, 2017.
- [32] R. Zhao, X. Ma, J. Xu, and Q. Zhang, "Removal of the pesticide imidacloprid from aqueous solution by biochar derived from peanut shell," *Bioresources*, vol. 13, no. 3, pp. 5656–5669, 2018.
- [33] S. G. Mohammad, S. M. Ahmed, A. E.-G. E. Amr, and A. H. Kamel, "Porous activated carbon from lignocellulosic agricultural waste for the removal of acetamiprid pesticide from aqueous solutions," *Molecules*, vol. 25, no. 10, p. 2339, 2020.
- [34] Z. Xu *et al.*, "Understanding reactions and pore-forming mechanisms between waste cotton woven and FeCl₃ during the synthesis of magnetic activated carbon," *Chemosphere*, vol. 241, p. 125120, 2020.
- [35] G. Liu *et al.*, "Metal–organic framework preparation using magnetic graphene oxide– β -cyclodextrin for neonicotinoid pesticide adsorption and removal," *Carbohydr Polym*, vol. 175, pp. 584–591, 2017.
- [36] S. M. de Oliveira Brito, H. M. C. Andrade, L. F. Soares, and R. P. de Azevedo, "Brazil nut shells as a new biosorbent to remove methylene blue and indigo carmine from aqueous solutions," *J Hazard Mater*, vol. 174, no. 1–3, pp. 84–92, 2010.
- [37] A. K. Verma, R. R. Dash, and P. Bhunia, "A review on chemical coagulation/flocculation technologies for removal of colour from textile wastewaters," *J Environ Manage*, vol. 93, no. 1, pp. 154–168, 2012.
- [38] N. Das and R. K. Jana, "Adsorption of some bivalent heavy metal ions from aqueous solutions by manganese nodule leached residues," *J Colloid Interface Sci*, vol. 293, no. 2, pp. 253–262, 2006.
- [39] M. R. Fouad, "Validation of adsorption-desorption kinetic models for fipronil and thiamethoxam agrichemicals on three types of Egyptian soils," *Egypt J Chem*, vol. 66, no. 4, pp. 219–222, 2023.
- [40] Y. S. Ho, J. C. Y. Ng, and G. McKay, "Kinetics of pollutant sorption by biosorbents," *Separation and purification methods*, vol. 29, no. 2, pp. 189–232, 2000.
- [41] C. Li, T. Lou, X. Yan, Y. Long, G. Cui, and X. Wang, "Fabrication of pure chitosan nanofibrous membranes as effective absorbent for dye removal," *Int J Biol Macromol*, vol. 106, pp. 768–774, 2018.